Numerical modelling of self-desiccation of hardening cement paste

E. A. B. Koenders
Heerema Elevated Infrastructure b.v.
Rotterdam, The Netherlands

K. van Breugel
Delft University of Technology, Department of Civil Engineering, Section for Concrete Structures,
Delft, The Netherlands

In this paper a numerical model is presented with which it is possible to predict the non-thermal hydration-induced volume changes that develop during hardening of a cement-based material. The model equilibrates the relative humidity in the pore system with the free surface energy in hardening cement past. From a certain state of equilibrium, the deformation of a cementitious material can be determined. The numerical simulations are in good agreement with a limited number of experimental results considered in this paper.

Key words: **Modelling, pore structure, self-desiccation, autogenous shrinkage, cement hydration**

1 Introduction

1.1 General

In the design of civil structures, durability is gaining more and more the interest of the construction principals. The way how to realize a durable structure can be categorised roughly into two main disciplines. At first, designers and engineers have to design a building project in such a way, that the desired lifetime of this project is guaranteed. This can be considered as the designers approach. At a conference in Brisbane in Australia, Somerville [24] called this: *Durability by design*.
Secondly, the quality of the building material plays an important role. In order to achieve a durable structure with low maintenance costs, the material of which the structure is made must satisfy certain quality requirements. If the building material is concrete, the demands on quality of the concrete microstructure are of paramount importance.

In order to meet the increasing higher demands on the material level, new types of concrete have been developed. This led to the introduction of special types of concrete with improved material properties which are expected to be more durable. Generally, these types of concrete are called: high performance concretes (HPC) or high strength concretes (HSC). Although the material properties of these types of concrete, generally, show a substantial improvement in comparison with conventional concretes, these types of concrete also have some properties that require due attention.

In many high quality concretes, which often have a low w/c ratio, substantial volume changes may occur during hardening of the material. This type of volume change is called: *autogenous shrinkage*. This autogenous shrinkage is, in a way, caused by changes in the state of the water in the gradually emptied pore space (see Fig. 1). For low water/cement ratio mixes, the autogenous shrinkage strains may exceed the maximum tensile strain capacity of the concrete (0.1 á 0.2‰, see Fig. 2). Any restraint of the deformations will induce stresses in the hardening concrete. This may cause cracking of the concrete which may jeopardise the durability of structures. Therefore, although the structure is designed correctly and the load bearing capacity is sufficient, a substantial reduction of durability may be introduced by the deformations, stresses and cracks which develop during hardening of the concrete. For example, large macro or micro-cracks may serve as "canals" for transport of chloride ions from the concrete's surface via the "damaged" microstructure to the reinforcement. Generally, this reduction of quality of a concrete structure can be considered as self-destruction of the hardening microstructure that is caused by a mechanism that acts from the "inside". Most annoying in this respect is the fact that for a given mixture these volumetric changes, as they develop during the hardening process, can not be influenced from the exterior. The contributions of the individual mix-components determine this mechanism. A change of the contributions of the different mix components or a variation of the properties of these components will directly affect the volume changes of the hardening material. To which extent the contributions of the individual mix components influence this volumetric change of the hardening microstructure is still unclear. As yet, there is no clear quantitative description of the mechanism behind this type of volumetric contraction. i.e. autogenous shrinkage, of the hardening microstructure.

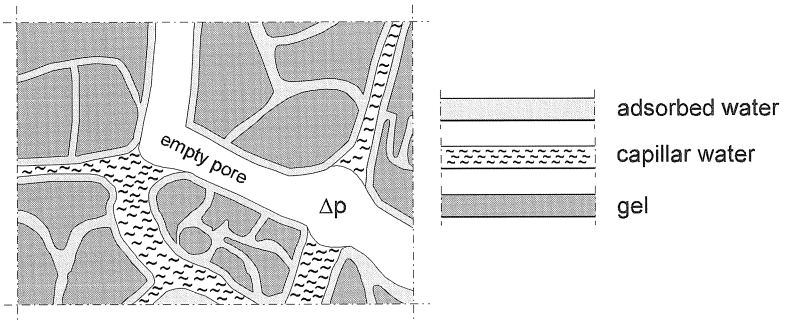

Fig. 1. *Schematical presentation of the microstructure of a cement paste. Reduction of relative humidity in the pore.*

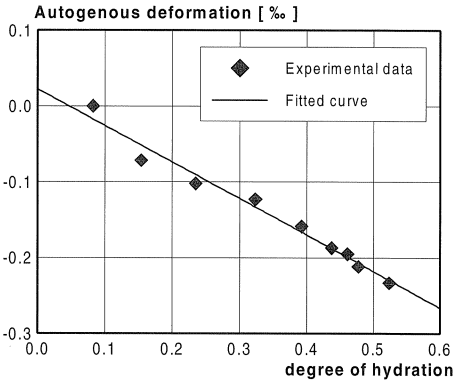

Fig. 2. Autogenous shrinkage of a HSC *as a function of the degree of hydration (w/c=0.3, T=20°C) [15].*

1.2 *Research aims*

The main goal of this research project on volume changes in hardening concrete was to explore the possibility to describe the main mechanism behind the process that causes the non-thermal, hydration-induced volume changes of hardening cement-based materials and to develop a numerical model for simulating these volume changes quantitatively. For the time being, emphasis will be on isothermally cured concrete. This is in order to avoid complicating factors related to temperature effects on the microstructure, i.e. on the pore structure.

The development of numerical tools for the evaluation of the hardening properties of concrete structures will contribute to a reliable assessment of the quality of concrete structures. In order to develop a model that is consistent and reliable, it is encouraged to descend from the macro-scale to the micro-scale level. Modelling physical and chemical processes at this particular level may contribute to a better understanding of the material behaviour that is generally observed at the macro-scale level.

1.3 *Outline of the paper*

In the next section a model is discussed with which the pore structure of a hardening cement paste can be described. A reliable description of the pore structure is inevitable for calculating the thermodynamic equilibrium in the pore system. The theory behind this thermodynamics-based model is briefly dealt with in section 3. For more detailed background information reference is made to the work of Defay et al. [9], and more in particular to Setzer [1972, 1976, 1978]. From this state of equilibrium, the non-thermal hydration induced deformations can be determined (autogenous shrinkage). The way how this is modelled is described in section 4. The potential of the model to predict the autogenous shrinkage of hardening cement paste is presented in section 5. The paper ends with conclusions (see E.A.B. Koenders [16]).

The hydration process, which is assumed to be the driving force behind the non-thermal hydration induced deformation mechanism is determined numerically with the HYMOSTRUC model. HYMOSTRUC

is a numerical simulation program with the potential to simulate and predict hydration curves as a function of the particle size distribution and chemical composition of the cement, the water/cement ratio and the temperature [6] (see also HERON Vol. 37 no. 3).

2 Pore structure

2.1 *Classification of pores*

The pore volume of cement paste is generally defined as the initial paste volume minus the volume of the solid material. The ratio between the pore volume and the initial paste volume is defined as the porosity. For cement paste, it is generally assumed that these pores exhibit a continuous pore size distribution [6]. For neat cement paste, the pore system consist of pores with diameters that range between 10 Å to 10^7 Å [32]. The pore diameters involved in the pore size distribution of a cement-based material can be subdivided into different categories that characterise a certain type of porosity. These are the *gel pores, the capillary pores* and the *air voids*. Several authors have proposed upper and lower boundaries for these three types of pores. However, no general agreement exists about the border limits that should be applied. As an example, in Table 1, limits as proposed by Young [32] are given.

For the proposed classification of pores, only the pores within the range of the capillary pores are considered to be capable to transport water or gas through the hardening microstructure.

The diameter of the capillary pores range from 0.002 μm ≤ ϕ ≤ 10 μm, where ϕ is the pore diameter.

The porosity and the pore size distribution are effected by several factors. These are the water/cement ratio, the degree of hydration, the curing temperature, the cement composition and the particle size distribution of the cement.

2.2 *Modelling the pore size distribution*

During the hydration process the cement paste changes gradually from a "liquid" into a hardened porous material. During hardening, the pore size distribution changes as well. The pore size distribution of a cementitious material can either be measured by, for example, mercury intrusion, or be obtained by numerical simulations. In Fig. 3 (left), a typical pore size distribution is presented for three cement pastes with different water/cement ratios. It can be seen that the capillary pore volume is larger for pastes with a higher water/cement ratio.

The cumulative pore size distribution for the capillary pore water can be described mathematically with the expression (see Fig. 3) [6]:

$$\frac{V_{por}}{V} = a \ln\left(\frac{\phi}{\phi_0}\right) \tag{1}$$

where V_{por} is the pore volume, ϕ the diameter of the capillary pore, ϕ_0 the minimum capillary pore diameter and "a" a *pore structure constant*. The pore volume formed by pores smaller than ϕ_0 = 0.002 μm (see Table 1), i.e. gel porosity, is not included in this formulation.

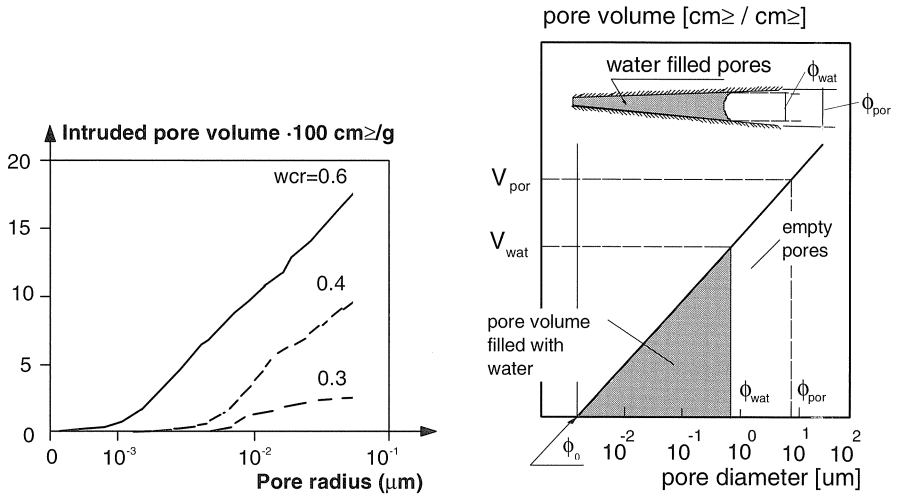

Fig. 3. Left: Effect of water/cement ratio on the cumulative pore size distribution [20]. Right: Schematical representation of the pore size distribution with indication of the location of the pore water in the pore volume (after [6]).

The total pore volume in a certain cement paste depends on the state of the hydration process, viz. the degree of hydration α. At the initial stage of the hardening process the total pore volume is equal to the paste volume minus the volume of cement. This ratio is determined by the water/cement ratio. At that particular stage, the total pore volume is completely filled with water[1]. After some hydration has occurred (α>0), the capillary pore volume has decreased due to the formation of hydration products. The pores do not remain completely filled with water since some part of the water volume has been used up by the reaction with cement. The pores with the largest diameter are emptied first. From this, a distinction can be made between pores that are still completely filled with water, $\leq\phi_{wat}$, and empty pores. The diameter of the pore that is still completely filled with water will be within the border limits of the capillary pores, e.g. $\phi_0 < \phi_{wat} < \phi_{por}$, where ϕ_{por} is the maximum pore diameter of the pore size distribution. This maximum pore diameter can be derived from equation (1). At a certain degree of hydration, the maximum pore diameter involved in the pore system can be determined with:

$$\phi_{por}(\alpha(t)) = \phi_0 \exp\left(\frac{1}{a}\frac{V_{por}(\alpha(t))}{V}\right) \qquad (2)$$

[1] The dissolved gas in the capillary pore water is disregarded.

Table 1. Classification of pores in cement paste (after [32]).

Classification of pores in cement paste			
Type	Diameter [_m]	Description	Role of water (adopted in model)
Air voids	>10	Entrained air	No transport of water or gas.
Capillary pores	10–0.002	Meso-macro pores	Able to transport water or gas.
Gel pores	< 0.002	Micro pores	No transport of water or gas

The actual total pore volume $V_{por}(\alpha(t))$ changes continuously throughout the hardening process. The pore space will reduce due to the formation of hydration products but, on the other hand, new pore space will be formed due to the volumetric reduction that is a result of the chemical reaction between the water and the cement (chemical or "Le Chatelier" shrinkage). Therefore, in this equation the total pore space $V_{por}(\alpha(t))$ is considered to be built up from two contributions. These are the actual pore volume that is occupied currently by capillary water and an additional volume that is the result of the chemical shrinkage. The relative contributions of both volumes change continuously during the hydration process. The changes of the total pore volume are accompanied by changes of the pore wall area.

The pore wall area of the hardening cement paste is considered to be covered by a thin adsorption layer of water molecules. The thickness of this layer mainly depends on the relative humidity in the pore system [13]. Changes of the actual water volume in the system due to hydration will change the relative humidity in the pore space and, therefore, also affect the thickness of this adsorption layer. It is assumed that the water volume that is accommodated in the adsorption layer goes at the cost of the free capillary pore water volume that is available for further hydration. Therefore, the diameter of the pore that is still completely filled with water will become smaller due to adsorption of water at the pore wall area.

When adopting the modelling approach as it is proposed up till now, detailed information on the properties of pore structure of a hardening cement paste is available. The only parameter in eq. (1) that is unknown is the pore structure constant "a". The value of this unknown parameter can be determined either by using experimental data or by numerical models. Book keeping a data-base that contains information on the pore structure of different types of mixtures is a serious option to achieve an adequate prediction of the pore structure constant "a". Using a numerical model to generate information on the pore structure constant "a" is even more convenient and more challenging. In the next section it will be elucidated how the pore structure constant "a" can be determined from pore size distribution measurements. In addition, in section 2.4, it will be outlined how this constant can be determined by numerically modelling.

2.3 *Pore structure constant "a" determined from experiments*

It is possible to determine the pore structure constant "a" from pore size distribution measurements. The dimensionless parameter "a" can be derived by dividing the total pore volume that is measured by mercury intrusion by the corresponding pore range according to the formula:

$$a = \frac{V_{por}}{V \cdot \ln(\phi/\phi_0)} \tag{3}$$

The diameter of the smallest capillary pore ϕ_0 is equal to 0.002 µm. In equation (3), the pore diameter ϕ is equal to the largest pore diameter. From literature it was found that the pore structure constant ranges roughly between 0.05 (coarse cement) and 0.15 (fine cement) [12, 8, 18, 27]. The exact value depends on, among other parameters, the type and fineness of the cement that is used. From Fig. 4 it can be seen that the relationship between the total pore volume and the corresponding pore size distribution can be described with curves with a pore structure constant which is almost constant throughout the whole hardening process. This permits the use of a constant value for the pore structure constant "a" for the simulations of the pore structure during the whole hardening process.

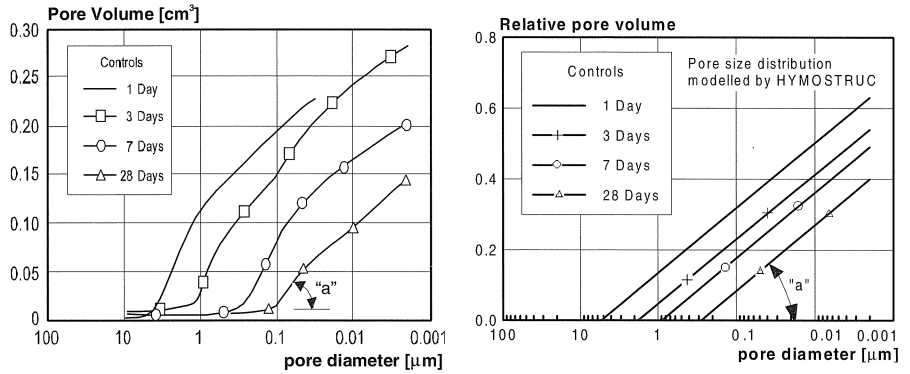

Fig. 4. Left: Pore size distribution measured by Whiting [26], Right: Pore size distribution according to HYMOSTRUC *(eq. (1) (for* HYMOSTRUC *see* HERON *Vol. 37, no. 3).*

With the proposed procedure it is easy to determine a pore structure constant "a" from pore size distribution measurements. In Fig. 4 pore size distribution measurements (left hand side) are compared with the pore size distribution as modelled according to equation (1) (right hand side). From the measurements presented in this example, a pore structure constant "a" of about 0.08 could be calculated. The simulated pore size distribution (Fig. 4, right) shows the reduction of the total pore volume and the maximum pore diameter with progress of the hydration process (see also Fig. 3). Whether the pores are filled with water or empty depends on the degree of hydration, at least in case of sealed curing.

2.4 *Pore structure constant "a" determined from random particle structure*

In the previous section 2.3 the pore structure constant was determined from experimental results. In this section, it will be elucidated how similar results can be obtained from numerical simulations with the "extended" HYMOSTRUC model. In the extended version of the HYMOSTRUC model, the formation of microstructure is modelled by an increase of the radii of the spherical cement particles that are *randomly* parked in space. During hydration, the cement particles start to grow or "expand" while forming a microstructure. Some particles may become embedded in the outer product layer of larger particles. In Fig. 5 two stages of the hydration process are presented for a cement of medium fineness (Blaine 420 m^2/kg) and a water/cement ratio of 0.3. Initially, when no hydration has taken place, only unhydrated cement particles exist which are distributed randomly in the water. At a degree of hydration of 0.1, a microstructure with little formation of hydration products can be observed. Note that a distinction is made between the hydration products formed inside the original grain boundary, called 'inner product' and outside this boundary, called "outer product". At a degree of hydration of 0.5, the actually developed hydration products tend to form a dense microstructure. From this structure, the pore space can be recognised (black background colour). Most of the pores are closed and surrounded by expanded cement particles. The average dimensions of the pores that can be observed range roughly between 1 and 10 μm. Since the shape of the pores are rather irregular, is it hard to determine a pore size distribution from this microstructural model. To overcome this, use can be made of the weighted average of the total pore volume and total pore wall area, i.e. the hydraulic radius. Among others, Setzer [21] proposed a procedure to determine the hydraulic radius from the ratio between the total pore volume V_{por} and the total pore wall area A_{por}.

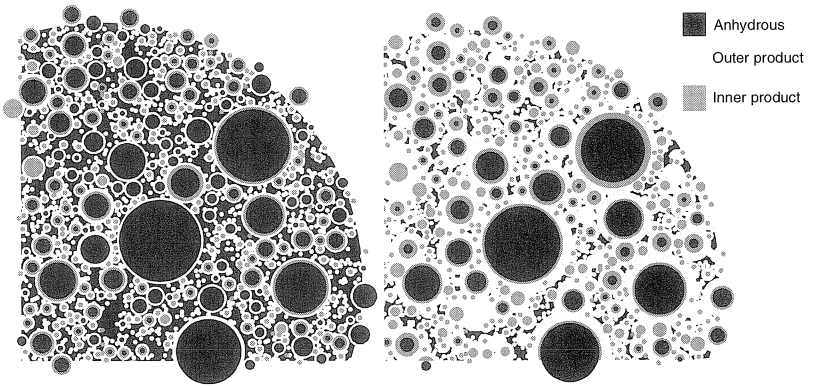

Fig. 5. Cross-section of a random particle structure at $\alpha = 0.1$ (left) and $\alpha = 0.5$ (right). Representing a cement paste of medium fineness (Blaine 420 m^2/kg) and a water/cement ratio of 0.3. (background colour black)

This hydraulic radius R_H, is defined as follows:

$$R_H = \frac{V_{por}}{A_{por}} \tag{4}$$

For an arbitrary "slice" of a random particle structure, the pore volume V_{por} can be determined by subtracting the area that is covered by the expanding cement particles from the total cross-sectional area of the slice and multiplied by the thickness of the slice. The pore wall area can be determined by adding up all those parts of the circumference of the growing cement particles (outer product), which directly border the pore space and multiply this total pore circumference by the thickness of the slice.
With equation (4), the hydraulic radius can be determined for the random particle structure (shown in Fig. 5). The hydraulic radius changes continuously during the hardening process. It decreases with increasing degree of hydration. This appears to be true for the three types of cement with different fineness which are considered in Fig. 6 (left). The figure also shows that the hydraulic radius is inversely proportional with the fineness of the cement.

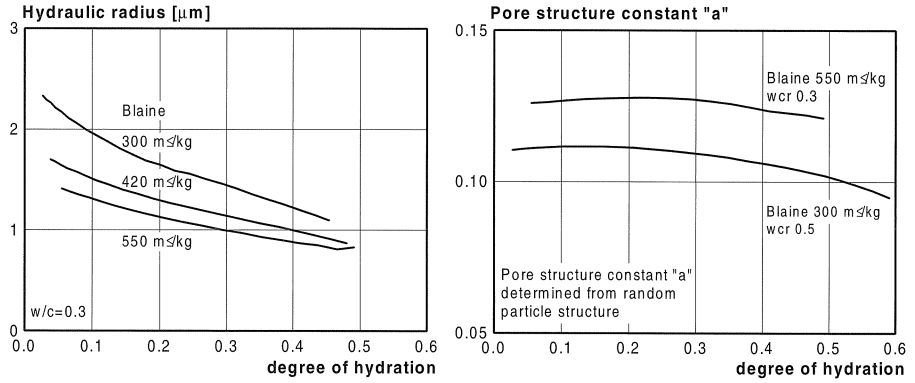

Fig. 6. Left: Hydraulic radius (eq. (4)) vs degree of hydration, Right: Pore structure constant "a" versus degree of hydration for two different cement pastes determined from the random particle structure.

Densification of the microstructure due to the formation of hydration products around the hydrating cement particles will reduce the initial pore volume of the hardening cement paste. On the other hand, it will enlarge the pore wall area. Assuming that the hydraulic radius represents the weighted pore diameter for the hardening paste, the pore constant "a" can be determined from a random particle structure. From the hydraulic radius R_H and the pore volume V_{por}, the pore structure constant "a" can be calculated with equation (1) with $\phi = 2R_H$ and $\phi_0 = 0.002$ µm. In Fig. 6 (right), the pore structure constant is shown for two different types of cement paste. It appears that the value of "a" changes only slightly for both pastes with progress of the hydration process. The value is highest for the cement paste that contains fine cement and a low water/cement ratio. A higher value "a" in equation (1) implies that more smaller pores are involved in the microstructure. The same trend is generally found in experimental data [10].

3 Analysis of thermodynamic equilibrium in the pore system

After mixing, a cement paste consists only of a water-cement dispersion. At this early stage of hardening, cement grains are randomly distributed through the paste and no structure has been formed yet. This means that all pores in the paste are considered to be completely filled with water. After setting, at a certain stage of the hydration process, pores are partly filled with water.
The empty pore volume is filled with water vapour. Based on internal energy balance, a thin layer of water molecules is adsorbed at the pore walls. There exists a water / vapour interface between the adsorbed water and the air in the empty pores and between the capillary water and the air in the empty pores. In general, this system can be considered as a three phase system, e.g. adsorbed water – interface layer – air (gas). As hydration proceeds, the thickness of the adsorption layer will change. Changes in the thickness of the adsorption layer determine the changes in the surface energy of the gel particles. These changes are accompanied by external volume changes.

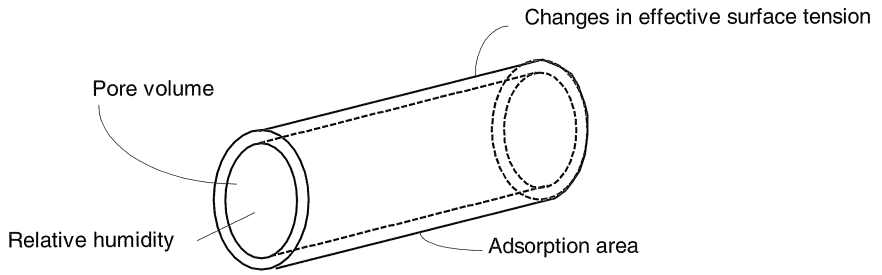

Fig. 7. Schematic representation of a pore with an adsorbed layer.

After a proposal by Setzer [21], in this paper only the change of the surface energy at the pore walls of the empty pores will be considered in the model to describe the thermodynamic equilibrium in the pore system. The capillary surface tension in the dividing surface between the gas phase and the capillary water is not considered.
For the relationship between the changes in the effective surface tension, σ, and the thickness of the adsorption layer $\Gamma(p_g/p_0)$ at a certain relative humidity p_g/p_0, it holds [22, 23, 30, 21, 19]:

$$\sigma = RT \int_{p_g/p_0}^{p_g/p_0 = 1} \Gamma d(\ln(p_g/p_0)) \tag{5}$$

For a hardening cement paste, the change of the relative humidity in the empty pore space is driven by the hydration process. Since the relative humidity affects the number of mono-molecular layers adsorbed to the pore walls, the surface energy of the hardening cement paste will also be affected. Equation (5) describes the "effective surface energy σ" that remains after the number of mono molecular layers at the pore walls has changed due to a change of the relative humidity in the empty pores. Several authors [21,30] have used different symbols in their papers to indicate this change of the surface energy as described with equation (5). Instead of σ as applied in equation (5),

also $\Delta\gamma$ or ΔF are used. All notations are, in fact, applied to describe the same mechanism, viz. the change of the surface energy in the system.

3.1 *Adsorption layer at the pore wall area*

Due to the existence of adhesion forces [7], vapour molecules tend to be adsorbed at the surface of a pore wall of a porous material. Generally, the thickness of this adsorption layer is restricted. The adsorbed molecules are in thermodynamic equilibrium with the gas phase in the empty pore space. At the same time, the amount of adsorbed molecules is determined by the relative vapour pressure in the gas, i.e. the relative humidity. At decreasing relative humidity, water molecules will desorb from the surface layer. The effective surface energy σ at the pore walls will change when the thickness of the adsorption layer Γ (see eq. 5) changes. As the thickness of the adsorption layer is a function of the relative humidity, a change in it will affect the thickness of the adsorption layer as well as the effective surface energy. The relationship between the thickness of the adsorption layer and the relative humidity in the pore system has been investigated by several authors [17, 1, 9, 13]. In [17], Hagymassy describes the thickness of the adsorption layer in terms of the number of mono-molecular layers (Fig. 8). At a relative pore pressure of 1.0 about 6 mono-molecular layers are adsorbed to the pore walls. Considering the thickness of one mono-layer to be equal to 3 Å, the thickness of an adsorption layer can reach a maximum thickness up to 18 Å. This order of magnitude of thickness of the adsorption layer has also been found by Badmann et.al. [2]. In [7], Cuperus visualised the adsorption layer by application of ultra filtration technique in combination with SEM scanning. With this technique he could measure the thickness of the adsorption layers ranging from 20 Å to about 30 Å.

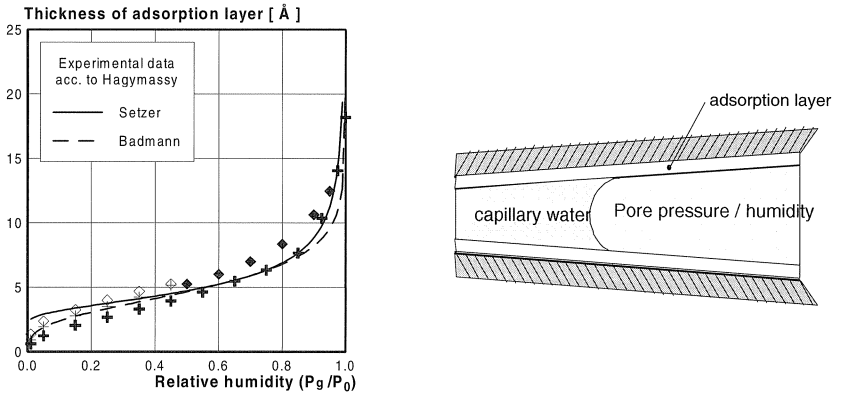

Fig. 8. Left: Thickness of the adsorption layer at the pore walls in the pore system as measured by Hagymassy [13]. Right: Schematical representation of the pore system.

3.2 *Relative humidity in empty pore space*

Directly after setting the microstructure of a hardening cement paste starts to develop. This is accompanied by the development of a pore structure. Initially, the relative humidity in the pore system (space) is equal to 100%. With progress of the hydration process, water is consumed by the anhydrous cement to form new hydration products. Due to this process, parts of the pores remain

filled with capillary water and parts of the pores become empty. At this stage of hardening, the relative humidity in the empty pore space will drop below 100%. In HYMOSTRUC, the relative humidity RH = p_g/p_0 in the empty pore space is modelled according to the Kelvin equation [12, 9] for tubular shaped pores in the form as used by Grün et. al. [12]:

$$\ln(\mathrm{RH}) = \ln\left(\frac{p_g}{p_0}\right) = \frac{-4\sigma}{RT\gamma_w\phi_{wat}} \tag{6}$$

in which ϕ_{wat} is the largest pore diameter that is still completely filled with water (see Fig. 3, right) and σ the surface tension of water. Instead of the surface tension of water the effective surface tension σ will be used here as described by equation (5) (after Setzer [21]).
The Kelvin equation describes the correlation between the relative humidity as a function of the pore diameter ϕ_{wat} and the effective surface energy σ. Both the pore diameter ϕ_{wat} and the effective surface energy σ will change as hydration proceeds, at least in so far the hydration process causes changes in the relative humidity in the pore system.

In Fig. 9 results are shown of the changes of the relative humidity in the hardening cement paste as calculated with the HYMOSTRUC model. The relative humidity in the pore system is presented for three different water/cement ratios and for three different finenesses of the cement. According to the results shown in Fig. 9, the relative humidity ranges between 100% and 75% for hydration times up to 1000 hours. The results are in reasonable agreement with results measured by other authors, for example Wittman [29] and Baroghel-Bouny [33]. They also measured that the relative humidity of hardening cement paste ranges between the 100% and about 70%.

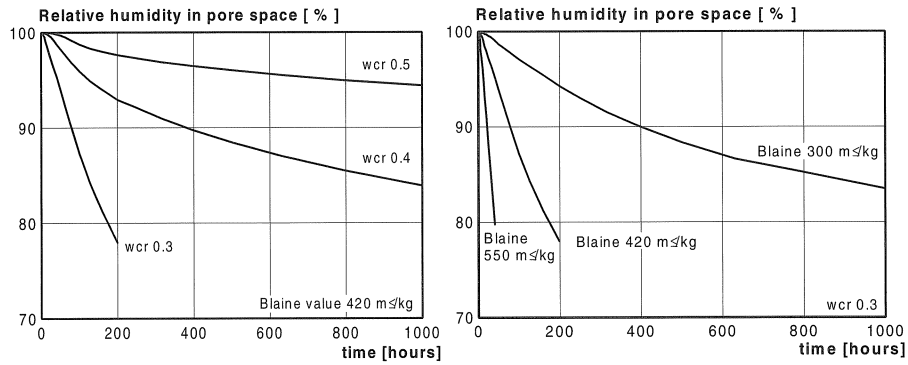

Fig. 9. Relative humidity in the empty pore space versus time. Left: Three different water/cement ratios. Right: Three different finenesses of the cement.

4 Deformation of the cement paste due to self-desiccation

4.1 *Deformation mechanism*

It was Bangham [3] who related the external deformation of coal to the change of the surface energy. In several papers [4, 3, 5] Bangham applied the adsorption equation of Gibbs to describe this phenomenon. Bangham used his theory to point out that with solid surfaces, as opposed to liquid surfaces, the surface energy, representing the work spent for the formation of a unit of new surface, must be in thermodynamic equilibrium with the pressure. In his work, he considered a three-phase system as mentioned in section 3.1. He found that the expansion of coal could be related linearly to changes in the internal surface energy with increasing thickness of the adsorption layer. This approach has been shown valid for hardened cement paste by, among others, Wittmann [29]. It is noticed that the Bangham equation has a semi-phenomenological basis and should not be considered as a physical law. This should be born in mind when it is proposed to apply a modified Bangham for quantification of the deformational behaviour of hardening cement-based systems in which the relative humidity is beyond the range considered by Bangham, which was up to about 40%.

When dealing with hardening cement paste, the material properties change continuously with progress of the hydration process. Therefore, the relationship between the external deformation and the changes in effective surface energy must be considered incrementally and can be formulated as:

$$\frac{\partial \varepsilon_a(\alpha(t))}{\partial \alpha} = \lambda \cdot \frac{\partial \sigma(\alpha(t))}{\partial \alpha} \tag{7}$$

where $\partial\varepsilon_a(\alpha(t))$ is the strain increment that describes the microstructural deformation of the hardening paste (autogenous shrinkage due to self-desiccation), $\partial\sigma(\alpha(t))$ the change of the effective surface energy (see eq. (5)) and λ a proportionality factor. In fact, this proportionality factor is the compliance modulus of the hardening material, e.g. cement paste.
The proportionality factor λ, that relates the microstructural deformation to the changes in of the surface energy, has been discussed by several authors [5, 31, 14, 19]. Minor differences appear between the relations as proposed by these authors. According to Bangham [5], this constitutive relation has the following shape:

$$\lambda = \frac{\Sigma \cdot \rho}{3E} \tag{8}$$

where Σ is the pore wall area per unit weight (adsorption surface), ρ the density of the material and E the Young's modulus. In [30], Wittmann used a similar relation to model the swelling deformation of hardened cement paste. In his model, the pore wall area Σ, the density ρ and the Youngs modulus are taken as constants. For hardening cement paste, however, these parameters can not be considered as constant values. The parameters change throughout the hardening process.
Therefore, the relation (8) has to be modified in order to be applicable for modelling volumetric changes of hardening cement-based materials. In this respect the pore wall area requires due attention. As hydration proceeds, pores will be emptied. This implies that a certain part of the pore wall area borders on the capillary pore water (filled pores) and a remaining part borders on gas

phase (empty pores). Only the pore wall area of the empty pores will be considered in the description of the volumetric changes of the adsorption area. This is also required from a thermodynamic point of view, since the load that acts on the microstructure from the interior, is exerted by the effective surface tension in the adsorption area [21]. Therefore, the proposed constitutive equation has the following shape.

$$\lambda(\alpha, \mathrm{RH}, wcr) = \frac{(A_{\mathrm{por}}(\alpha) - A_{\mathrm{wat}}(\alpha, \mathrm{RH})) \cdot \rho_{\mathrm{pa}}(wcr)}{3 \cdot E_{\mathrm{p}}(\alpha)} \tag{9}$$

where:

$A_{por}(\alpha) - A_{wat}(\alpha,RH)$ = pore wall area of the empty pores (adsorption area)
$\rho_{pa}(wcr)$ = specific mass of the cement paste
$E_p(\alpha)$ = modulus of elasticity of the cement paste

As can be seen from the constitutive relation (9) the proportionality factor depends on the degree of hydration and the water/cement ratio. Also the relative humidity plays a role, as it determines the thickness of the adsorption layer and hence also the magnitude of A_{wat}.

For a detailed description of the formulation of the pore wall area of the empty pores and the modulus of elasticity of the hardening cement paste, reference is made to [16].

5 Experiments versus numerical simulations

5.1 *Description of the experiments*

An experimental program was conducted with the aim to validate the numerical model with which the autogenous deformation of hardening cement paste due to self-desiccation can be calculated. As far as the water/cement ratio is concerned, cement pastes with w/c ratios of 0.3, 0.4 and 0.5 are considered in this paper. For the fineness of the cement, Blaine values of 420 and 550 m^2/kg are considered in the experiments. All experiments were carried out under isothermal conditions at 20°C. This temperature was imposed to the specimen with the help of two cryostats. Minor differences between the desired temperature (20°C) and the measured temperature appeared during hardening process. The effect of these temperature differences on the autogenous deformation measurements was compensated afterwards. However, the differences appeared to be very small (± 2°C).

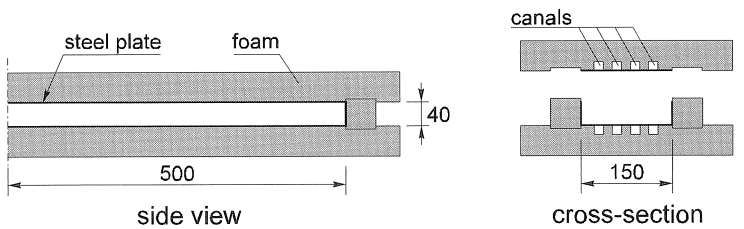

Fig. 10. Schematic representation of the thermally insulated mould.

The autogenous deformation is measured from large specimens cast in a temperature controlled mould. The inner dimensions of the mould are 1000 x 150 x 40 mm^3 (Fig. 10). The mould can be dismantled into several parts. These parts are made of 40 mm foam plastic with a low coefficient of thermal conductivity ($\lambda = 0.03$ W/m^2K). On one side a 1 mm thick steel plate is glued to the foam to ensure a smooth surface and to cover the "canals" that are cut in the foam. These canals enable cooling or heating of the concrete surface. The canals are connected to a cryostat, one cryostat for the top part of the mould and an other cryostat for the bottom part of the mould. Both cryostats control the water temperature and pump the water through the canals. During hardening, the temperature and the load-independent deformation of the paste are measured. The deformations of the cement paste are measured with LVDT's on two sides exterior of the mould, over a length of 750 mm between two steel bars (that pass through the mould) which are embedded in the paste during casting. As soon as the setting period of the paste has ended, measurements can start.

5.2 *Degree of hydration*

From the experimental set-up, the autogenous deformation is measured as a function of time. These results are compared with the simulated results calculated with the model proposed in the sections 3 and 4 of this paper. The progress of the hydration process, one of the main parameters in the model, is determined by the HYMOSTRUC model simultaneously. Therefore, it is also possible to relate the measured autogenous deformation to the degree of hydration.

5.1 *Cement of high fineness (Blaine 550 m^2/kg)*

On the left hand side of Fig. 11 the autogenous deformation is presented as a function of time. It concerns a neat Portland cement paste that contains a cement of high fineness (Blaine 550 m^2/kg). The results are shown for three different water/cement ratios. These are 0.3, 0.4 and 0.5. The results show a strong increase of the autogenous deformation with decreasing water/cement ratio. The largest autogenous shrinkage strain, ca. 2‰, is measured after about 80 hours of hardening for a cement paste with a water/cement ratio of 0.3. The measurements show a strong increase of the autogenous deformation directly after setting. For a cement paste with a water/cement ratio of 0.4, less shrinkage is measured. Again, the increase of the autogenous deformation proceeds very rapidly. After 160 hours of hydration a shrinkage of 1‰ is reached. This is a large reduction ($\approx$ 50%) in comparison with the cement paste with a water/cement ratio of 0.3. A further increase of the water/cement ratio to 0.5 reduces the autogenous shrinkage by another 50%. After 160 hours of hardening, a shrinkage of about 0.5‰ is measured. The measured autogenous deformation is simulated with the proposed model. The measurements are in good agreement with the numerical simulations. This holds true for all the three water/cement ratio's that are considered.

On the right hand side of Fig. 11, the autogenous deformation is presented as a function of the degree of hydration. The results are presented for the same three Portland cement pastes as were considered at the left hand side of Fig. 11. From the figure it can be seen that the autogenous deformation of the hardening cement paste is driven by the hydration process. For all three water/cement ratios, the numerical simulations are in good agreement with the experimentally obtained results (Fig. 11, right).

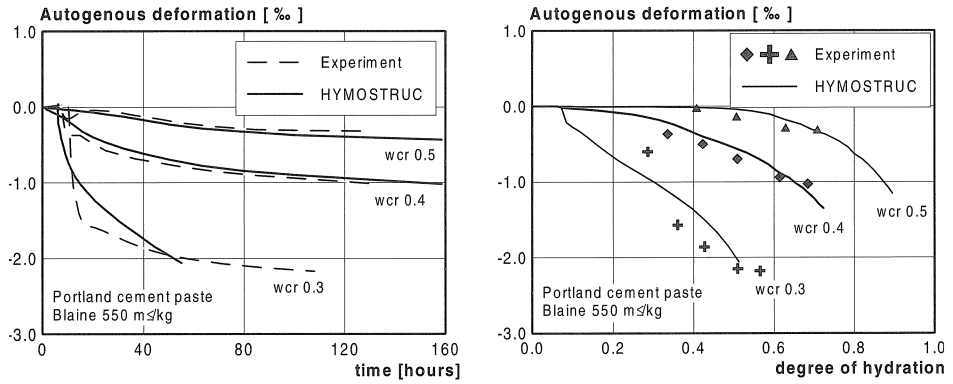

Fig. 11. Left: Autogenous shrinkage versus time. Right: Autogenous shrinkage versus degree of hydration. Portland cement paste (different water/cement ratios).

The degree of hydration reached at cessation of the hydration process is lower for the cement pastes with a lower water/cement ratio. Less water is available to continue the hydration process. However, from the results in Fig. 11 it appears that the autogenous deformation is inversely proportional to this effect. For low water/cement ratio pastes. e.g. *wcr* = 0.3, the maximum pore diameter of capillary pores that are still completely filled with water is much smaller than the maximum pore diameter of a cement paste with a higher water/cement ratio (e.g. *wcr* 0.5). This phenomenon is accompanied by a lower relative humidity (see Fig. 12) in the emptied pore space and introduces a larger change of the surface energy. This results in larger deformations of the microstructure (eq. (5) and (9)). The thermodynamic equilibrium in the pore system governs this process.

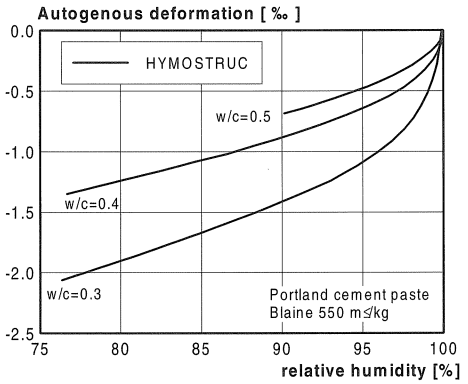

Fig. 12. Autogenous shrinkage versus relative humidity in the empty pore space (self-desiccation).

5.4 *Cement of medium fineness (Blaine 420 m^2/kg)*

On the left hand side of Fig. 13, the measured autogenous deformation is compared with numerical simulations that were carried out with HYMOSTRUC. It concerns the measured deformation versus time for a Portland cement paste and a water/cement ratio of 0.3 and 0.4. Good agreement is reached between the measurements and the numerical simulations. This holds for both water/cement ratios. The experimental measurements, as well as the numerical simulations, show an equal tendency for the relationship between the development of the autogenous deformation and the water/cement ratio.

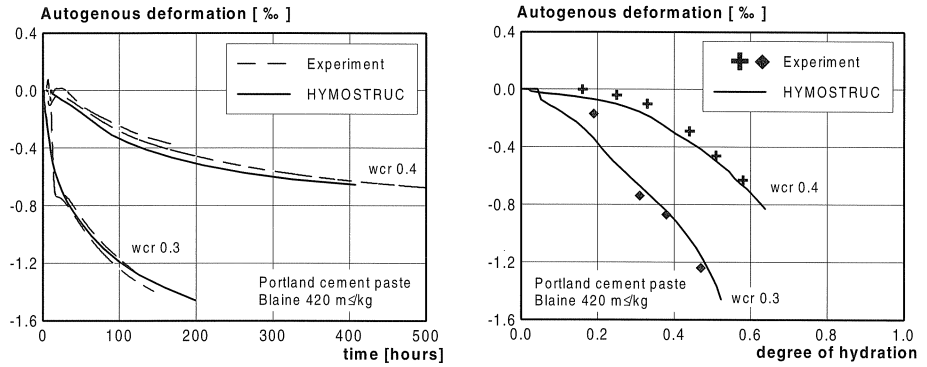

Fig. 13. Left: Autogenous shrinkage versus time. Right: Autogenous shrinkage versus degree of hydration. Portland cement paste (different water/cement ratios).

If the water/cement ratio increases, the autogenous deformation decreases. Increasing the water/cement ratio from 0.3 to 0.4 results in a reduction of the autogenous deformation from 1.2 ‰ to 0.38 ‰ after 100 hours of hardening. This absolute difference appears to increase with elapse of time. At the right hand side of Fig. 13, the autogenous deformation of the hardening cement paste is presented as a function of the degree of hydration. The experimental results are compared with the numerical simulations as calculated by the proposed model.

5.5 *Numerical simulations versus literature data*

In [25], Tazawa et. al. published an extensive experimental study on autogenous deformation of cementitious material. Some of these results are simulated with the HYMOSTRUC model. It concerns a cement paste with a water/cement ratio of 0.23 and another paste with a water/cement ratio of 0.3. Both mixtures did not exhibit swelling. The results are shown in Fig. 14. Good agreement has been obtained between the measurements and the numerical simulations. This appeared to be true for both the paste with a water/cement ratio of 0.3 and for the paste with a water/cement ratio of 0.23. For the paste with a water/cement ratio of 0.3, the autogenous deformation reaches a value of about 1.5‰ after about 50 days of hardening, while for the cement paste with a water/ cement ratio of 0.23 the autogenous deformation reached a value of about 2.5‰. This order of magnitude was also calculated with the HYMOSTRUC model.

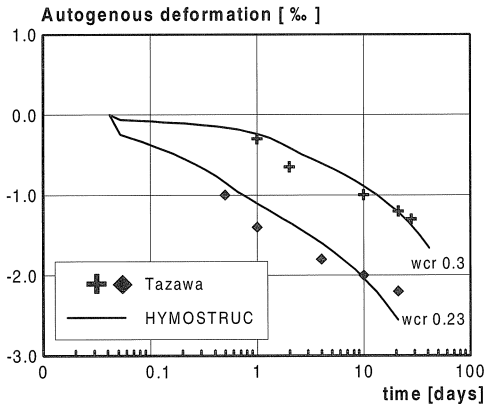

Fig. 14. Comparison between experiments on cement paste (Blaine 352 m^2/kg) carried out by Tazawa et. al. and numerical simulations by HYMOSTRUC.

6 Conclusions

In this paper, a numerical model is proposed which has the potential to simulate the volume changes of hardening cement-based materials. Emphasis was on the effect of changes in the effective surface energy in the gradually drying system. The model heavely draws on some views concerning the thermodynamic equilibrium in a pore systems as proposed by Setzer (1972, 1978). For determination of the deformations a modified Bangham equation was used. A major modification was that allowance was made for the changes in the adsorption area during hydration. This was achieved by adopting a proportionality factor for relating the deformations of the system with changes in the effective surface energy that was a function of the gradually changing adsorption area. A satisfactory agreement was obtained between the numerical simulations and the experimental results concerning autogenous shrinkage. The promising results constitute a challenge for further research in the chosen direction. Major challenges concern further investigation of the role of other phenomena which are considered to play a role in the volume changes at early ages, e.g. the capillary tension and disjoining pressure. These phenomena were not considered so far, maily because of the fact that the ideas put forward by Setzer provided us already with a workable basis for numerical modelling.

In another HERON edition the potential of the approach followed in this paper will be discussed in view of simulating moisture transport within an hydrating paste. This moisture transport is caused by differences in the (local) water/cement ratio in the interfacial zone and the bulk paste .

7 References

[1] Amberg, C.H. and Mc. Intosh, R. (1952), A Study of Adsorption Hysteresis by means of Length Changes of a Rod of Porous Glass, Canadian Journal of Chemistry 4, 30, 1012.

[2] Badmann, R. et. al. (1981), J. Coll. Int. Sci,Vol. 82, pp. 534-542.

[3] Bangham, D.H. (1937), The Gibbs Adsorption Equation and Absorption on Solids, London, Gurney and Jackson.

[4] Bangham, D. H. and Fakhoury, N. (1931), The Swelling of Charcoal, Royal Society of London , CXXX, 81-89.

[5] Bangham, D.H. and Maggs, F.A.P. (1944), The Strength and Elastic Constants of Coal in Relation to their Ultra-fine Structure, The British Coal Utilisation Research Association, The Royal Institution, London,

[6] Breugel, K. van, (1991), Simulation of hydration and formation of structure in hardening cement-based materials, Faculty of Civil Engineering, Delft, Delft University of Technology, pp. 295, PhD.

[7] Cuperus, F. P., (1990), Characterisation of Ultrafiltration Members, Pore Structure and Top Layer Thickness, Enschede, University of Twente, pp. 103, PhD.

[8] Day, R.L. and Marsh, B. K. (1988), Measurement of Porosity in Blended Cement Pastes, Cement and Concrete Research ,Vol 18, pp. 63-73.

[9] Defay, R. Prigogine, I. and Bellemans, A. (1966), Surface Tension and Adsorption, London, Longmans London.

[10] Feldman, R.F. and Cheng-yi, H. (1985), Cement, Silica Fume, Pastes, Porosity, Surface Properties, Secondary, Cement, Silica Fume, Pastes, Porosity, Surface Properties, 15, pp 766-774, 5.

[11] Goodrich, F.C., Rusanov, A.I., Sonntag, H. and Bülow, M. (1981), The modern Theory of Capillarity, Berlin, Akademie-Verlag.

[12] Grün, W. and Grün H.R. (1961), Zur Frage der Physikohemischen Verhaltensweise von Wasser des Hydratisierenden Zementes im Beton, Zement-Kalk-Gips, nr. 11, pp. 541-520.

[13] Hagymassy, J. Brunauer, JR. and Mikhail, R.Sh. (1969), Pore Structure Analysis by Water Vapor Adsorption, Journal of Colloid and and Interface Science, 29-3, pp. 485-491.

[14] Hiller, K.H. (1964), Strength Reduction and Length Changes in Porous Glass Caused by Water Vapor Adsorption, Journal of Applied Physics, 35, pp. 1622-1628.

[15] Koenders, E.AB. and Breugel, K. van (1995), The Effects of Autogenous Shrinkage on Cracking in Hardening High Strength Concrete, Concrete 95 Toward Better Concrete Structures, FIP-CIA, Brisbane Australia.

[16] Koenders, E.A.B., (1997), Simulation of Volume Changes in Hardening Cement-Based Materials, Faculty of Civil Engineering, Delft, The Netherlands, Delft University of Technology, pp. 171, PhD, ISBN 90-407-1499-1.

[17] Maggs, F.A.P. (1944), The Absolute Evaluation of Surface Areas of Solid Materials, Ultra-fine Structure of Coals & Cokes, The British Coal Utilisation Research Association, The Royal Institution, London.

[18] Moukwa, M. and Aitcin, P. C. (1988), The effect of Drying on Cement Pastes Pore Structure as Determined by Mercury Porosimetry, Cement and Concrete Research, Vol. 18, pp. 745-752.

[19] RAMACHANDRAN, V.S., FELDMAN, R.F. and BEAUDOIN, J.J. (1981), Concrete Science, Treatise on Current Research, Division of Building Research, National Research Council, Canada, Heyden.

[20] RENHE, Y., BAOYUAN, L. and ZHONGWEI, W. (1990), Study on Pore Structure of Hardened Cement Paste by SAXS, Cement and Concrete Research,Vol. 20, pp. 385-393.

[21] SETZER, M., J. (1978), Einfluss des Wassergehalts auf die Eigenschaften des erhärteten Betons, Deutscher Ausschuss Für Stahlbeton DAfSt ,Heft 280, pp. 43-79.

[22] SETZER, M. J., (1972), Oberflächenenergie und Mechanische Eigenschaften des Zementsteins, München, TU München, pp. 113, PhD.

[23] SETZER, M.J. (1976), A Method for Describtion of Mechanical Behaviour of Hardened Cement Paste by Evaluating Adsorption Data, Cement and Concrete Research, 6, 37-48.

[24] SOMERVILLE, G. (1995), Developments in Design and Performance Requirements for Post-Tensioned Bridges in the U.K., Concrete 95 Toward better concrete structures, Brisbane Australia.

[25] TAZAWA, E. and MIYAZAWA, S. (1992), Autogenous shrinkage caused by self desiccation in cementitious material, 9th Int. Conf. on Chemistry of Cement, New Delhi.

[26] WHITING, D. and KLINE, E. (1977), Pore size distribution in epoxy impregnated hardened cement pastes, Cement and Concrete Research,Vol. 7, pp 53-60.

[27] WINSLOW, D.L. (1990), The Pore Structure of Paste in Concrete, Cement and Concrete Research , Vol. 20, pp. 227-235.

[28] WISMAN, W.H. (1994), Introduction in Thermodynamics, Delft, Delft University Press.

[29] WITTMANN, F., (1968), Physikalische Messungen an Zementstein, München, TU München, Habilitationsshrift.

[30] WITTMANN, F.H. (1977), Grundlagen eines Modells zur Beschreibung charakterisstischer Eigenschaften des Betons, Deutscher Ausschuss Für Stahlbeton (Dafst), Heft 290,

[31] YATES, D. J. C. (1954), The Expansion of Porous Glass on the adsorption of Non-Polar Gases, Proceedings of the Royal Society of London ,224, 526-543.

[32] YOUNG, J.F., et.al., Materiaux et Construction, pp. 377-382.

[33] BAROGHEL-BOUNY, V., GODIN, J. and GAWSEWITCH, J., (1996), Proceedings of the 4th International Symposium on Utilization of High-strength/High-performance Concrete, pp 451-461, Paris.